Ultrahigh Quality Factor of a Levitated Nanomechanical Oscillator

Lorenzo Dania[1,*,§] Dmitry S. Bykov[1,†] Florian Goschin[1] Markus Teller[1,‡]
Abderrahmane Kassid[2] and Tracy E. Northup[1]

[1]*Institut für Experimentalphysik, Universität Innsbruck, Technikerstraße 25, 6020 Innsbruck, Austria*
[2]*Physics Department, Ecole Normale Supérieure, 24 rue Lhomond, 75005 Paris, France*

A levitated nanomechanical oscillator under ultrahigh vacuum is highly isolated from its environment. It has been predicted that this isolation leads to very low mechanical dissipation rates. However, a gap persists between predictions and experimental data. Here, we levitate a silica nanoparticle in a linear Paul trap at room temperature, at pressures as low as 7×10^{-11} mbar. We measure a dissipation rate of $2\pi \times 69(22)$ nHz, corresponding to a quality factor exceeding 10^{10}, more than 2 orders of magnitude higher than previously shown. A study of the pressure dependence of the particle's damping and heating rates provides insight into the relevant dissipation mechanisms.

The center-of-mass motion of a silica nanoparticle has recently been cooled to the quantum ground state [1–6], opening up the possibility to prepare nonclassical motional states of levitated objects consisting of billions of atoms [7]. However, a prerequisite to prepare and analyze such exotic states—and to exploit them for applications in sensing, transduction, or tests of fundamental physics—is a low-dissipation environment that preserves quantum coherence. For clamped nanomechanical oscillators, dissipation has been suppressed through engineering geometry and strain, resulting in quality factors above 10^{10} [8–11]. For levitated objects, in contrast, collisions with background-gas molecules are typically the dominant source of dissipation [12–14], and thus the route to suppressing dissipation lies not in materials engineering but in reducing the pressure. It has been estimated that damping rates of $2\pi \times 200$ nHz and quality factors of 3×10^{12} can be achieved in ultrahigh vacuum (UHV) [15].

Direct measurements of dissipation are crucial for levitated particles because additional heating and damping mechanisms become important as the pressure is reduced; it can no longer be assumed that gas damping dominates. Light scattering is of particular concern: for a particle confined in an optical tweezer, dissipation due to radiation damping already dominates over gas damping at high-vacuum pressures [16–19]. Quality factors of 10^8 have been reported for an optically trapped nanoparticle [20]. Electrical and magnetic traps are not compromised by light-induced decoherence, and for nanoparticles in such traps, quality factors of 2.6×10^7 and dissipation rates of $2\pi \times 0.59$ µHz have been reported [21–25].

Here, using a nanoparticle confined in a linear Paul trap in UHV, we measure an ultralow dissipation rate of $2\pi \times 69(22)$ nHz and a record quality factor of $1.8(6) \times 10^{10}$. These values pave the way for detection of forces and electric fields with sensitivities comparable to or surpassing the current benchmarks set by trapped atoms [26,27]. Moreover, the low pressure demonstrated here is a key condition to test wave-function-collapse models [28,29] and to engineer long-lived quantum states of motion of macroscopic mechanical oscillators [15,30,31]. In light of these goals, we characterize the noise environment in UHV, identifying the most likely noise sources.

Our primary goal is to investigate damping of the particle's motion as a function of pressure. Experiments are conducted in a vacuum chamber in which we vary the pressure from 7×10^{-11} mbar to 10^{-4} mbar. To increase the pressure from its minimum value, we limit the effective pumping speed of the chamber's combination pump (a nonevaporable getter and an ion pump) by partially closing a gate valve. With the valve fully closed, we reach 10^{-4} mbar in one day. To decrease the pressure back to UHV, we first reach 10^{-9} mbar with a turbomolecular pump. We then open the gate valve and pump with the combination pump to below 10^{-10} mbar. With this room-temperature setup, we expect that pressures one order of magnitude lower can be reached [32].

The silica particle used for the measurements presented here was loaded at 10^{-9} mbar via laser-induced acoustic desorption and temporal control of the Paul-trap potential [33]; these methods allow us to load particles over a range of pressures down to UHV. The particle has charge $q = +300(30)$ e and a nominal diameter of 300 nm; however, since we measure a mass $m = 4.3(4) \times 10^{-17}$ kg that is twice the mass of particles previously loaded from the same source [34,35], it is likely that the particle is a cluster of two nanospheres with a somewhat larger size. The particle's motion is detected optically [Fig. 1(a)]: a 780 nm laser beam with a power of 21 mW is focused with a waist of 300 µm on the particle; a lens collects the scattered light. Two methods are used to extract information from the collected light about
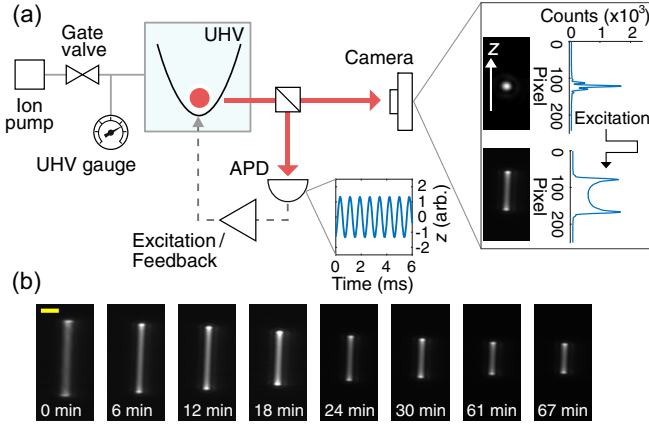
FIG. 1. Particle trapping and detection. (a) Schematic of the ultrahigh-vacuum (UHV) setup and detection schemes. A nanoparticle is detected in two ways: it is imaged with a camera, and its position is measured with an avalanche photodiode (APD) using a confocal technique. The camera inset shows particle images before and after excitation, as well as position histograms. The APD inset shows a time trace of the particle's position. (b) Camera snapshots of the particle with decaying oscillation amplitude at $P = 5.4 \times 10^{-8}$ mbar. Scale bar: 20 μm.

the particle's motion: confocal detection realized with a fiber-coupled avalanche photodiode (APD) [36–39], and imaging of the particle on a CMOS camera [24]. We use the APD method to track the particle's position in real time. A typical APD signal is shown in an inset of Fig. 1(a). With the camera, we measure the oscillation amplitude averaged over the camera acquisition time. Compared to the APD method, the camera method has lower spatial and temporal resolution but offers a larger field of view, allowing us to measure particle amplitudes up to hundreds of micrometers. Moreover, the camera detection is more resilient to drifts in the optics alignment and laser power, making it possible to perform days-long measurements.

To modify the particle's motion, we apply electrical forces by supplying a suitable voltage to the trap electrodes [34]. To reduce the particle's amplitude, we apply feedback based on the real-time APD detection; to increase the amplitude, we apply a sinusoidal driving force at the mechanical resonance frequency of the trapped particle. An inset in Fig. 1(a) shows images of the feedback-cooled particle and the driven particle.

For measurements of the particle's damping, we focus on motion along the trap's z axis, for which dc voltages provide confinement. We choose this axis because here the particle is less susceptible to noise of the ac trap drive [40]. The equation of motion $\ddot{z} + \gamma\dot{z} + \Omega_z^2 z = (1/m)\mathcal{F}_{\text{th}}$ [41] describes the particle's position, where γ is the damping rate, which is proportional to the background pressure P [13,19]; $\Omega_z/2\pi = 1.28$ kHz is the oscillation frequency; and $\mathcal{F}_{\text{th}}$ is the stochastic force due to thermalization with the environment. Here we assume that $\mathcal{F}_{\text{th}}$ dominates over all other stochastic forces, such as those due to laser, electronic, and displacement noise.

We determine γ using two methods. The first method, ring-down, consists of measuring the amplitude relaxation

$$\langle z(t)^2 \rangle = \langle z(0)^2 \rangle e^{-\gamma t}, \quad (1)$$

where Eq. (1) holds when the viscous force dominates over $\mathcal{F}_{\text{th}}$, such that the particle follows a deterministic trajectory. Figure 1(b) shows images from a relaxation experiment. While a particle with large motional amplitude is prone to trap anharmonicities, the ring-down method is insensitive to them [42]. The second method, ring-up, consists of preparing the particle at a low temperature T_{fb} via feedback cooling, then switching off cooling and measuring the particle's thermalization with background gas at room temperature T_0. When $\mathcal{F}_{\text{th}}$ dominates over the viscous force, the particle follows a stochastic trajectory in time. Averaging over an ensemble of such trajectories allows us to obtain the mean energy [41]

$$\langle E(t) \rangle = k_{\text{B}} T_0 + k_{\text{B}} (T_{\text{fb}} - T_0) e^{-\gamma t}, \quad (2)$$

from which we extract γ. We use the ring-down method because it allows us to characterize the damped harmonic oscillator in a single measurement. We use the ring-up method for two reasons: first, a fit to Eq. (2) for data taken under low vacuum (i.e., in thermal equilibrium) establishes a calibration between the APD voltage and the energy $k_{\text{B}} T_0$. We use this calibration to obtain T_{fb} [43]. Second, we compare the heating rate determined from the ring-up method with the rate expected from thermal noise, in order to determine whether nonthermal noise sources play a significant role at UHV.

In a first set of measurements, we analyze how γ changes when P is varied. We extract γ with a ring-up measurement at $P_1 = 1.2 \times 10^{-4}$ mbar and with ring-down measurements at $P_2 = 5.4 \times 10^{-8}$ mbar, $P_3 = 5 \times 10^{-9}$ mbar, and $P_4 = 7 \times 10^{-11}$ mbar. At P_1, the particle is prepared at $T_{\text{fb}} = 1$ K and monitored with the APD during thermalization for 10 s. This sequence is repeated 400 times. For each repetition, we square the position data and average them over 0.1 s. This procedure determines the particle's energy with a 10 Hz sampling rate, much faster than the expected ring-up rate of $\sim 10^{-2}$ Hz. In Fig. 2(a), we plot the energy traces together with their ensemble average. We then fit the ensemble average with Eq. (2), under the assumption that the particle thermalizes at $T_0 = 300$ K [23,33,41]. From this fit, we extract $\gamma_{P_1} = 2\pi \times 37(9)$ mHz.

For the ring-down measurements at pressures P_2, P_3, and P_4, the particle's motion is initially excited to an amplitude of hundreds of microns, and the subsequent relaxation is measured with gated camera imaging. The particle is illuminated only for the camera measurement time, 1 s for each acquisition, so that the particle's motion is minimally influenced by the laser, e.g., due to radiation damping or force noise induced by power fluctuations [19].
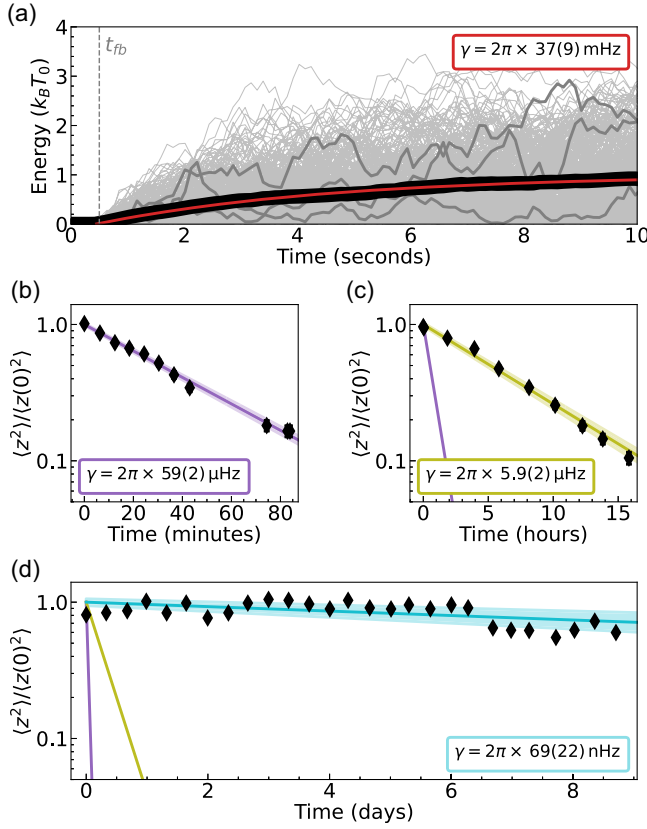
FIG. 2. Measurements of the damping rate γ. (a) Ring-up measurement at $P_1 = 1.2 \times 10^{-4}$ mbar. Gray: 400 individual data traces. Three examples are highlighted in dark gray. Black: ensemble average. Red: fit of the ensemble-averaged data with Eq. (2), where T_{fb} is fixed to 1 K. The dashed line $t = t_{\mathrm{fb}} = 0.5$ s indicates the time at which feedback cooling is switched off. (b) Ring-down measurement at $P_2 = 5.4 \times 10^{-8}$ mbar, (c) $P_3 = 5 \times 10^{-9}$ mbar, and (d) $P_4 = 7 \times 10^{-11}$ mbar, with a logarithmic scale used for the ordinate axis. Error bars on the data are smaller than the diamond symbols; they correspond to the uncertainty in determining amplitudes from camera images. Solid lines represent fits with Eq. (1) in logarithmic scale, with $\langle z(0)^2 \rangle$ and γ as fit parameters. Light shaded regions indicate 1σ error bars on fit parameters. Fits for higher pressures are reproduced in the lower-pressure plots for comparison.

Figures 2(b)–2(d) show the normalized squared amplitude of the particle's motion as a function of time, measured at P_2, P_3, and P_4. A fit of the data with Eq. (1) yields $\gamma_{P_2} = 2\pi \times 59(2)$ μHz, $\gamma_{P_3} = 2\pi \times 5.9(2)$ μHz and $\gamma_{P_4} = 2\pi \times 69(22)$ nHz. At the lowest pressure, P_4, the uncertainties associated with camera detection are much smaller than the residuals of the exponential fit, indicating that Eq. (1) does not fully capture the particle's dynamics [43]. This would occur if the viscous force were not dominant. The viscous force is 3 orders of magnitude larger than $\mathcal{F}_{\mathrm{th}}$ under the assumption that $\mathcal{F}_{\mathrm{th}}$ is due to background-gas collisions at room temperature. However, we cannot rule out the possibility that $\mathcal{F}_{\mathrm{th}}$ is dominant: under high vacuum, the
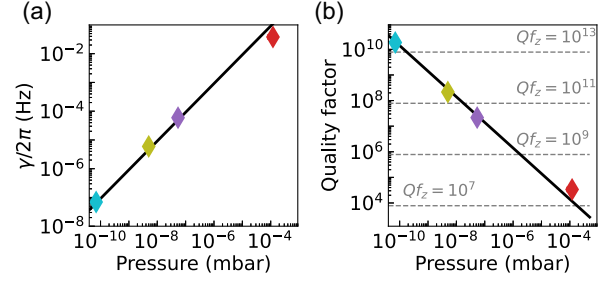

FIG. 3. Quality factor of the levitated oscillator. (a) Damping rate γ as a function of pressure. Error bars for γ represent the uncertainty of the fit parameter, while error bars for pressure represent the imprecision of the pressure gauge. Error bars are smaller than the diamond symbols. Colors indicate the corresponding fits in Fig. 2. The solid line shows a linear fit $\gamma/(2\pi) = aP$ to the data in logarithmic scale, where the parameter a depends on the particle and the background gas properties [13,19]. Since non-negligible uncertainties are present in both γ and P, we use a total least squares regression to fit the data [51]. The fit yields $a = 0.9(2)$ kHz mbar^{-1}. See Ref. [43] for a comparison with theory. (b) Quality factor at four pressures. Error bars are propagated from the uncertainties of γ shown in (a). The solid line represents the function $Q = \Omega_z/(2\pi aP)$, where a is obtained from the fit in (a). Dashed lines indicate values for the product Qf_z, where $f_z = \Omega_z/(2\pi)$ is the oscillation frequency.

equilibrium temperature of a nanoparticle in a Paul trap has been shown to vary inversely with pressure due to noise on the trap electrodes [23]; furthermore, the noise seen by a particle oscillating over hundreds of micrometers may be significantly higher than for a localized particle [52]. A second possibility is that the particle's dynamics were disrupted by infrequent spikes in electronic or vibrational noise, which could explain the bimodal distribution of the residuals.

In Fig. 3(a), we plot γ determined from the fits of Fig. 2 for different pressures. The data are consistent with a linear model $\gamma \propto P$, from which we infer that at pressures as low as P_4, damping is still dominated by background-gas collisions. In Fig. 3(b), we plot the quality factors $Q = \Omega_z/\gamma$. The highest value for Q, obtained at P_4, is $1.8(6) \times 10^{10}$, corresponding to $2.4(7) \times 10^{13}$ for the Q-frequency product, a benchmark for optomechanics in the quantum regime [53]. A second set of data at P_4 yields $Q = 3(2) \times 10^{10}$ for different trap parameters [43].

The ultrahigh quality factors and low dissipation demonstrated here open up the possibility to use levitated particles in Paul traps for force sensing and tests of quantum mechanics. For such applications, it is important to quantify both the frequency stability and the heating rate of the nanoparticle oscillator in UHV. To this end, we calculate the Allan deviation to characterize the frequency stability. We record a time trace of the particle's position for $t_{\mathrm{f}} = 600$ s and extract the particle frequency as a function of time via a phase-locked loop in postprocessing. For this measurement, the particle evolves freely in the Paul-trap
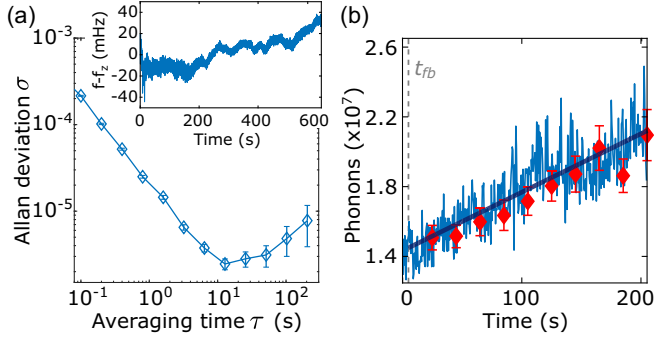
FIG. 4. (a) Allan deviation of the particle oscillation frequency at pressure P_4. Lines connect neighboring data points. Error bars represent the standard error of the frequency mean. Inset: frequency drift as a function of time. (b) Heating-rate measurements at P_4 for continuous (blue) and stroboscopic (red) illumination of the particle with the detection laser. Error bars on the stroboscopic measurements represent the standard deviation of individual temperature measurements. The dashed line $t = t_{fb} = 5$ s indicates the time at which feedback cooling is switched off. The dark-blue line is a fit to the data for continuous illumination, the slope of which yields the heating rate $\Gamma_{tot} = 3.3(2) \times 10^4$ phonon/s. The fit for stroboscopic illumination is not shown since it coincides with the fit for the continuous case.

potential at pressure P_4. From the discrete frequency time trace, we determine the Allan deviation as

$$\sigma(\tau) = \left[\frac{1}{2f_z^2} \frac{1}{N(\tau) - 1} \sum_{k=2}^{N(\tau)} (\bar{f}_k - \bar{f}_{k-1})^2 \right]^{1/2}, \quad (3)$$

with $\bar{f}_z = \Omega_z/(2\pi)$; $N(\tau) = [t_f/\tau]$ the number of intervals, where $[a/b]$ represents integer division; and $\bar{f}_k$ the average frequency in the kth interval of duration τ. The results are shown in Fig. 4(a). For an optimum averaging time $\tau_{opt} = 20$ s, a fractional frequency fluctuation of $\sigma(\tau_{opt}) = 2 \times 10^{-6}$ is achieved. For comparison, one expects a thermally limited value [54] of $\sigma(\tau_{opt}) = 1/\sqrt{Q\Omega_z\tau_{opt}} = 2 \times 10^{-8}$, which we do not reach due to inefficient detection [55] and mechanical frequency fluctuations. For larger values of τ, σ increases due to drifts of the particle's frequency. We extract a linear drift rate of $\sim 8 \times 10^{-8}$ Hz s^{-1}. Possible causes of the drift include nonlinearities of the confining potential, fluctuations in trap-electrode voltages, and fluctuations in the detection-laser power.

In a final set of measurements, we determine the nanoparticle's heating rate to quantify the noise environment, which is assumed to be white over the ultranarrow bandwidth of the oscillator. We carry out a ring-up measurement at P_4: The particle is prepared at $T_{fb} = 0.8$ K, which we assume corresponds to a thermal state. Next, feedback cooling is turned off and the particle's position is monitored for 200 s with continuous laser illumination. This sequence is repeated

100 times. As the $1/e$ ring-up time expected from γ_{P4} is approximately one month, we expand Eq. (2) to first order in time

$$\langle E(t) \rangle = k_B T_{fb} + k_B (T_0 - T_{fb}) \gamma t$$
$$\approx k_B T_{fb} + k_B T_0 \gamma t, \quad (4)$$

which corresponds to a heating rate $\Gamma_{gas} = k_B T_0 \gamma / (\hbar \Omega_z)$, assuming that the force noise is dominated by gas collisions. From the averaged data [Fig. 4(b)], we extract a rate $\Gamma_{meas}^{bright} = 3.3(2) \times 10^4$ phonon/s. In comparison, our ring-down measurement predicts a rate $\Gamma_{gas} = k_B T_0 \gamma_{P4}/(\hbar \Omega_z) = 2.1 \times 10^3$ phonon/s, 16 times smaller than our measured value.

From the ring-up measurement, we infer that background-gas recoil is not the dominant noise source. One possible noise source is the detection laser; to exclude this, we rerun the heating-rate experiment in the dark. In this case, the laser is turned on only during the first 5 s of each ring-up in order to initialize the particle via feedback cooling, and for 500 ms every 20 s in order to stroboscopically measure the particle's energy during its free evolution. The results of this measurement are also plotted in Fig. 4(b); we extract a rate $\Gamma_{meas}^{dark} = 3.1(8) \times 10^4$ phonon/s, consistent with the rate determined under continuous illumination, from which we deduce that the laser does not play a significant role.

A second possible stochastic-force source is electric-field noise, due to fluctuations in ac and dc drive fields, Johnson noise, or coupling between the particle's secular motion and micromotion. From Γ_{meas}^{dark}, we extract a white force-noise spectrum $S_{ff} = 4m\hbar\Omega_z\Gamma_{meas}^{dark} = 4 \times 10^{-42}$ N^2 Hz^{-1} acting on the particle. If S_{ff} is dominated by electric-field noise, we can determine the electric-field-noise spectrum: $S_{EE} = S_{ff}/q^2 = 1.7 \times 10^{-9}$ (V/m)^2 Hz^{-1}, equivalent to an electronics voltage noise of $S_v = d\sqrt{S_{EE}} = 38$ nV/$\sqrt{\text{Hz}}$, where $d = 0.92$ mm is the particle-to-electrode distance. For comparison, Vinante et al. estimate that $S_v = 10$ nV/$\sqrt{\text{Hz}}$ is around the threshold of what can be achieved without extraordinary engineering efforts [29]. Thus, if the electric field is the dominant noise source, we have room for improvement. But reducing S_v to this threshold value would still yield a heating rate slightly larger than Γ_{gas}; to suppress electric-field noise further—in particular, for future experiments at even lower pressures—we could reduce q.

A third possibility is displacement noise due to trap vibrations. If S_{ff} is dominated by displacement noise [56], we infer a vibration energy density $S_{zz} = 2\hbar\Gamma_{meas}^{dark}/(\pi m \Omega_z^3) = 9.5 \times 10^{-26}$ m^{2}Hz^{-1}. We have measured S_{zz} at the vacuum chamber to be 2×10^{-25} m^2 Hz^{-1}, suggesting that displacement noise may be dominant [43]. To discriminate between electric and displacement noise, it will be sufficient to study the dependence of Γ_{meas}^{dark} on q, since Γ_{meas}^{dark} is independent of q for displacement noise. It has been argued

that vibrational noise can be suppressed to negligible values in experiments with levitated nanoparticles [29]. Two other possible noise sources are discussed in Ref. [43].

In conclusion, with a levitated nanoparticle, we have realized a mechanical oscillator with a quality factor of $1.8(6) \times 10^{10}$, determined from the damping rate of the particle's oscillations at 7×10^{-11} mbar. At this pressure, the calculated collision rate with background-gas molecules is 1.1 kHz, that is, on average, one molecule collides with the particle every 1.2 oscillation cycles. For levitated optomechanical experiments in the quantum regime, it will be necessary to operate at similar or lower pressures [29,31,56–58], which is facilitated by the direct loading method demonstrated here. While the measured damping rates are consistent with a gas-damping model [13,19], the measured heating rates are higher than expected solely from interaction with the background gas; we have identified the most likely noise sources and routes to address them.

One application of this work is ultrasensitive force detection [7,26]: Force-noise and damping-rate measurements in UHV will allow wave-function-collapse models to be tested in unexplored regimes [23,59,60]. Pulsed-measurement schemes such as the one adopted here will be necessary to exploit these high quality factors. Furthermore, if we introduce self-homodyne detection [35] and cold damping, we expect to prepare the particle's motional ground state within the dark potential of the electrodynamic trap, enabling tests of quantum physics in the absence of photon recoil.

Source data are available on Zenodo [61].

[*]ldania@ethz.ch

[†]dmitry.bykov@uibk.ac.at

[‡]Present address: ICFO-Institut de Ciencies Fotoniques, The Barcelona Institute of Science and Technology, 08860 Castelldefels (Barcelona), Spain.

[§]Present address: Photonics Laboratory, ETH Zürich, CH-8093 Zürich, Switzerland.

[1] U. Delić, M. Reisenbauer, K. Dare, D. Grass, V. Vuletić, N. Kiesel, and M. Aspelmeyer, Cooling of a levitated nanoparticle to the motional quantum ground state, Science **367**, 892 (2020).

[2] L. Magrini, P. Rosenzweig, C. Bach, A. Deutschmann-Olek, S. G. Hofer, S. Hong, N. Kiesel, A. Kugi, and M. Aspelmeyer, Real-time optimal quantum control of mechanical motion at room temperature, Nature (London) **595**, 373 (2021).

[3] F. Tebbenjohanns, M. L. Mattana, M. Rossi, M. Frimmer, and L. Novotny, Quantum control of a nanoparticle optically levitated in cryogenic free space, Nature (London) **595**, 378 (2021).

[4] M. Kamba, R. Shimizu, and K. Aikawa, Optical cold damping of neutral nanoparticles near the ground state in an optical lattice, Opt. Express **30**, 26716 (2022).

[5] A. Ranfagni, K. Børkje, F. Marino, and F. Marin, Two-dimensional quantum motion of a levitated nanosphere, Phys. Rev. Res. **4**, 033051 (2022).

[6] J. Piotrowski, D. Windey, J. Vijayan, C. Gonzalez-Ballestero, A. de los Ríos Sommer, N. Meyer, R. Quidant, O. Romero-Isart, R. Reimann, and L. Novotny, Simultaneous ground-state cooling of two mechanical modes of a levitated nanoparticle, Nat. Phys. **19**, 1009 (2023).

[7] C. Gonzalez-Ballestero, M. Aspelmeyer, L. Novotny, R. Quidant, and O. Romero-Isart, Levitodynamics: Levitation and control of microscopic objects in vacuum, Science **374**, 168 (2021).

[8] Y. Tsaturyan, A. Barg, E. S. Polzik, and A. Schliesser, Ultracoherent nanomechanical resonators via soft clamping and dissipation dilution, Nat. Nanotechnol. **12**, 776 (2017).

[9] G. S. MacCabe, H. Ren, J. Luo, J. D. Cohen, H. Zhou, A. Sipahigil, M. Mirhosseini, and O. Painter, Nano-acoustic resonator with ultralong phonon lifetime, Science **370**, 840 (2020).

[10] A. Beccari, D. A. Visani, S. A. Fedorov, M. J. Bereyhi, V. Boureau, N. J. Engelsen, and T. J. Kippenberg, Strained crystalline nanomechanical resonators with quality factors above 10 billion, Nat. Phys. **18**, 436 (2022).

[11] M. J. Bereyhi, A. Arabmoheghi, A. Beccari, S. A. Fedorov, G. Huang, T. J. Kippenberg, and N. J. Engelsen, Perimeter modes of nanomechanical resonators exhibit quality factors exceeding 10^9 at room temperature, Phys. Rev. X **12**, 021036 (2022).

[12] P. S. Epstein, On the resistance experienced by spheres in their motion through gases, Phys. Rev. **23**, 710 (1924).

[13] S. A. Beresnev, V. G. Chernyak, and G. A. Fomyagin, Motion of a spherical particle in a rarefied gas. Part 2. Drag and thermal polarization, J. Fluid Mech. **219**, 405 (1990).

[14] A. Cavalleri, G. Ciani, R. Dolesi, M. Hueller, D. Nicolodi, D. Tombolato, S. Vitale, P. Wass, and W. Weber, Gas damping force noise on a macroscopic test body in an infinite gas reservoir, Phys. Lett. A **374**, 3365 (2010).

[15] D. E. Chang, C. A. Regal, S. B. Papp, D. J. Wilson, J. Ye, O. Painter, H. J. Kimble, and P. Zoller, Cavity opto-mechanics using an optically levitated nanosphere, Proc. Natl. Acad. Sci. U.S.A. **107**, 1005 (2010).

[16] A. Ashkin and J. M. Dziedzic, Optical levitation in high vacuum, Appl. Phys. Lett. **28**, 333 (1976).

[17] L. D. Hinkle and B. R. F. Kendall, Pressure-dependent damping of a particle levitated in vacuum, J. Vac. Sci. Technol. A **8**, 2802 (1990).

[18] T. Li, S. Kheifets, and M. G. Raizen, Millikelvin cooling of an optically trapped microsphere in vacuum, Nat. Phys. **7**, 527 (2011).

[19] V. Jain, J. Gieseler, C. Moritz, C. Dellago, R. Quidant, and L. Novotny, Direct measurement of photon recoil from a levitated nanoparticle, Phys. Rev. Lett. **116**, 243601 (2016).

[20] J. Gieseler, L. Novotny, and R. Quidant, Thermal nonlinearities in a nanomechanical oscillator, Nat. Phys. **9**, 806 (2013).

[21] B. R. Slezak, C. W. Lewandowski, J.-F. Hsu, and B. D'Urso, Cooling the motion of a silica microsphere in a magneto-gravitational trap in ultra-high vacuum, New J. Phys. **20**, 063028 (2018).

[22] A. Vinante, P. Falferi, G. Gasbarri, A. Setter, C. Timberlake, and H. Ulbricht, Ultralow mechanical damping with Meissner-levitated ferromagnetic microparticles, Phys. Rev. Appl. **13**, 064027 (2020).

[23] A. Pontin, N. P. Bullier, M. Toroš, and P. F. Barker, Ultranarrow-linewidth levitated nano-oscillator for testing dissipative wave-function collapse, Phys. Rev. Res. **2**, 023349 (2020).

[24] Y. Leng, R. Li, X. Kong, H. Xie, D. Zheng, P. Yin, F. Xiong, T. Wu, C.-K. Duan, Y. Du, Z. Q. Yin, P. Huang, and J. Du, Mechanical dissipation below 1 µHz with a cryogenic diamagnetic levitated micro-oscillator, Phys. Rev. Appl. **15**, 024061 (2021).

[25] J. Hofer, G. Higgins, H. Huebl, O. F. Kieler, R. Kleiner, D. Koelle, P. Schmidt, J. A. Slater, M. Trupke, K. Uhl, T. Weimann, W. Wieczorek, F. Wulschner, and M. Aspelmeyer, High-Q magnetic levitation and control of superconducting microspheres at millikelvin temperatures, Phys. Rev. Lett. **131**, 043603 (2023).

[26] J. Millen, T. S. Monteiro, R. Pettit, and A. N. Vamivakas, Optomechanics with levitated particles, Rep. Prog. Phys. **83**, 026401 (2020).

[27] D. C. Moore and A. A. Geraci, Searching for new physics using optically levitated sensors, Quantum Sci. Technol. **6**, 014008 (2021).

[28] D. Goldwater, M. Paternostro, and P. F. Barker, Testing wave-function-collapse models using parametric heating of a trapped nanosphere, Phys. Rev. A **94**, 010104(R) (2016).

[29] A. Vinante, A. Pontin, M. Rashid, M. Toroš, P. F. Barker, and H. Ulbricht, Testing collapse models with levitated nanoparticles: Detection challenge, Phys. Rev. A **100**, 012119 (2019).

[30] O. Romero-Isart, M. L. Juan, R. Quidant, and J. I. Cirac, Toward quantum superposition of living organisms, New J. Phys. **12**, 033015 (2010).

[31] O. Romero-Isart, A. C. Pflanzer, F. Blaser, R. Kaltenbaek, N. Kiesel, M. Aspelmeyer, and J. I. Cirac, Large quantum superpositions and interference of massive nanometer-sized objects, Phys. Rev. Lett. **107**, 020405 (2011).

[32] P. Obšil, A. Lešundák, T. Pham, K. Lakhmanskiy, L. Podhora, M. Oral, O. Číp, and L. Slodička, A room-temperature ion trapping apparatus with hydrogen partial pressure below 10^{-11} mbar, Rev. Sci. Instrum. **90**, 083201 (2019).

[33] D. S. Bykov, P. Mestres, L. Dania, L. Schmöger, and T. E. Northup, Direct loading of nanoparticles under high vacuum into a Paul trap for levitodynamical experiments, Appl. Phys. Lett. **115**, 034101 (2019).

[34] L. Dania, D. S. Bykov, M. Knoll, P. Mestres, and T. E. Northup, Optical and electrical feedback cooling of a silica nanoparticle levitated in a Paul trap, Phys. Rev. Res. **3**, 013018 (2021).

[35] L. Dania, K. Heidegger, D. S. Bykov, G. Cerchiari, G. Araneda, and T. E. Northup, Position measurement of a levitated nanoparticle via interference with its mirror image, Phys. Rev. Lett. **129**, 013601 (2022).

[36] A. N. Vamivakas, S. B. Ippolito, A. K. Swan, M. S. Ünlü, M. Dogan, E. R. Behringer, and B. B. Goldberg, Phase-sensitive detection of dipole radiation in a fiber-based high numerical aperture optical system, Opt. Lett. **32**, 970 (2007).

[37] S. Kuhn, P. Asenbaum, A. Kosloff, M. Sclafani, B. A. Stickler, S. Nimmrichter, K. Hornberger, O. Cheshnovsky, F. Patolsky, and M. Arndt, Cavity-assisted manipulation of freely rotating silicon nanorods in high vacuum, Nano Lett. **15**, 5604 (2015).

[38] F. Xiong, P. Yin, T. Wu, H. Xie, R. Li, Y. Leng, Y. Li, C. Duan, X. Kong, P. Huang, and J. Du, Lens-free optical detection of thermal motion of a submillimeter sphere diamagnetically levitated in high vacuum, Phys. Rev. Appl. **16**, L011003 (2021).

[39] D. S. Bykov, L. Dania, F. Goschin, and T. E. Northup, 3D sympathetic cooling and detection of levitated nanoparticles, Optica **10**, 438 (2023).

[40] C. Roos, T. Zeiger, H. Rohde, H. C. Nägerl, J. Eschner, D. Leibfried, F. Schmidt-Kaler, and R. Blatt, Quantum state engineering on an optical transition and decoherence in a Paul trap, Phys. Rev. Lett. **83**, 4713 (1999).

[41] J. Gieseler, R. Quidant, C. Dellago, and L. Novotny, Dynamic relaxation of a levitated nanoparticle from a non-equilibrium steady state, Nat. Nanotechnol. **9**, 358 (2014).

[42] B. C. Stipe, H. J. Mamin, T. D. Stowe, T. W. Kenny, and D. Rugar, Noncontact friction and force fluctuations between closely spaced bodies, Phys. Rev. Lett. **87**, 096801 (2001).

[43] See Supplemental Material at http://link.aps.org/supplemental/10.1103/PhysRevLett.132.133602 for the ion-trap geometry, detector calibration, a comparison of ring-down and ring-up measurements, analysis of residuals, discussions of noise due to electrode resistivity and coupling to rotational or librational modes, vibration measurements, analysis of the particle frequency, an estimate of the particle damping coefficient from theory, and additional ring-down data. The Supplemental Material includes Refs. [44–50].

[44] M. Brownnutt, M. Kumph, P. Rabl, and R. Blatt, Ion-trap measurements of electric-field noise near surfaces, Rev. Mod. Phys. **87**, 1419 (2015).

[45] L. Martinetz, K. Hornberger, and B. A. Stickler, Surface-induced decoherence and heating of charged particles, PRX Quantum **3**, 030327 (2022).

[46] D. R. Lide, *CRC Handbook of Chemistry and Physics*, 75th ed. (CRC Press, Boca Raton, 1995).

[47] M. Kumph, C. Henkel, P. Rabl, M. Brownnutt, and R. Blatt, Electric-field noise above a thin dielectric layer on metal electrodes, New J. Phys. **18**, 023020 (2016).

[48] B. E. Dahneke, Slip correction factors for nonspherical bodies—II free molecule flow, J. Aerosol Sci. **4**, 147 (1973).

[49] D. Ganta, E. Dale, J. Rezac, and A. Rosenberger, Optical method for measuring thermal accommodation coefficients using a whispering-gallery microresonator, J. Chem. Phys. **135** (2011).

[50] J. Millen, T. Deesuwan, P. Barker, and J. Anders, Nanoscale temperature measurements using non-equilibrium Brownian

dynamics of a levitated nanosphere, Nat. Nanotechnol. **9,** 425 (2014).

[51] G. H. Golub and C. F. van Loan, An analysis of the total least squares problem, SIAM J. Numer. Anal. **17,** 883 (1980).

[52] T. W. Penny, A low-noise electrically levitated oscillator for investigating fundamental physics, Ph.D. thesis, University College London, 2022.

[53] M. Aspelmeyer, T. J. Kippenberg, and F. Marquardt, Cavity optomechanics, Rev. Mod. Phys. **86,** 1391 (2014).

[54] E. Gavartin, P. Verlot, and T. J. Kippenberg, Stabilization of a linear nanomechanical oscillator to its thermodynamic limit, Nat. Commun. **4,** 2860 (2013).

[55] T. Manzaneque, M. K. Ghatkesar, F. Alijani, M. Xu, R. A. Norte, and P. G. Steeneken, Resolution limits of resonant sensors, Phys. Rev. Appl. **19,** 054074 (2023).

[56] T. Weiss, M. Roda-Llordes, E. Torrontegui, M. Aspelmeyer, and O. Romero-Isart, Large quantum delocalization of a levitated nanoparticle using optimal control: Applications for force sensing and entangling via weak forces, Phys. Rev. Lett. **127,** 023601 (2021).

[57] S. Bose, A. Mazumdar, G. W. Morley, H. Ulbricht, M. Toroš, M. Paternostro, A. A. Geraci, P. F. Barker, M. S. Kim, and G. Milburn, Spin entanglement witness for quantum gravity, Phys. Rev. Lett. **119,** 240401 (2017).

[58] L. Neumeier, M. A. Ciampini, O. Romero-Isart, M. Aspelmeyer, and N. Kiesel, Fast quantum interference of a nanoparticle via optical potential control, arXiv: 2207.12539.

[59] D. Zheng, Y. Leng, X. Kong, R. Li, Z. Wang, X. Luo, J. Zhao, C.-K. Duan, P. Huang, J. Du, M. Carlesso, and A. Bassi, Room temperature test of the continuous spontaneous localization model using a levitated micro-oscillator, Phys. Rev. Res. **2,** 013057 (2020).

[60] M. Carlesso, S. Donadi, L. Ferialdi, M. Paternostro, H. Ulbricht, and A. Bassi, Present status and future challenges of non-interferometric tests of collapse models, Nat. Phys. **18,** 243 (2022).

[61] L. Dania, D. S. Bykov, F. Goschin, M. Teller, A. Kassid, and T. E. Northrup, Data for Ultrahigh Quality Factor of a Levitated Nanomechanical Oscillator, v2, Zenodo (2024), 10.5281/zenodo.7819826.